Missouri University of Science and Technology

Scholars' Mine

International Specialty Conference on Cold-Formed Steel Structures

(1980) - 5th International Specialty Conference on Cold-Formed Steel Structures

Oct 18th, 12:00 AM

Simple Design Analysis of Lipped Channel Columns

J. Rhodes

J. Loughlan

Follow this and additional works at: https://scholarsmine.mst.edu/isccss

 Part of the Structural Engineering Commons

Recommended Citation

Rhodes, J. and Loughlan, J., "Simple Design Analysis of Lipped Channel Columns" (1980). *International Specialty Conference on Cold-Formed Steel Structures*. 1.
https://scholarsmine.mst.edu/isccss/5iccfss/5iccfss-session5/1

This Article - Conference proceedings is brought to you for free and open access by Scholars' Mine. It has been accepted for inclusion in International Specialty Conference on Cold-Formed Steel Structures by an authorized administrator of Scholars' Mine. This work is protected by U. S. Copyright Law. Unauthorized use including reproduction for redistribution requires the permission of the copyright holder. For more information, please contact scholarsmine@mst.edu.

SIMPLE DESIGN ANALYSIS OF LIPPED CHANNEL COLUMNS

by

J. Rhodes*
and
J. Loughlan**

Introduction

The effects of local buckling in the plate elements of a thin-walled column are known to substantially alter the subsequent column behaviour and the load-carrying capacity of the column. The interaction which occurs between the local buckling and overall column buckling is a complex phenomenon and has attracted the interest of many researchers, both from the purely analytical viewpoint (eg.(5)(10)) and from the design viewpoint (eg.(2)(6)(12)).

The major effects of local buckling are, (1) to reduce the compressional and flexural stiffnesses of the column, and (2) to change the effective geometry of the cross section, thus causing variation in the effective position of the neutral axis. Due to the latter effect an initially concentric load may become effectively eccentric after local buckling, and an initially eccentric load may effectively change its eccentricity. The combination of these effects leads to complicated analysis, and many of the design approaches proposed to deal with this problem reflect this complexity in the computational effort required.

In this paper a method is presented for the analysis of lipped channel columns under concentric or eccentric loading. The analysis can be carried out using a hand calculator or preferably a microcomputer and does not require any large scale computer use. Nevertheless, the method has been evolved on the basis of a rigorous theoretical approach which has been applied with highly accurate results to the analysis of stiffened plating (3)(4), plain channels (11), and lipped channels (7)(8), and describes the mechanics of column behaviour very adequately.

In the theoretical analyses mentioned above, rigorous analysis of the local buckling behaviour of the complete column cross-section was used. In the design approach presented here effective width expressions are used instead and the accuracy of the design predictions are dependent on the adequacy of the effective width expressions used.

---

* Senior Lecturer, University of Strathclyde, Dept. of Mechanics of Materials Montrose Street, Glasgow G1 1XJ, Scotland.

** Lecturer, Cranfield Institute of Technology, College of Aeronautics, Aircraft Design, Cranfield, Bedford MK43 0AL, England.

Outline of Theoretical Background

In the theoretical analysis a short section of the column is examined under an eccentric compression system as shown in Fig.1(a). It is assumed that at all stages in the post-local buckling range the tangent stiffness of the load-compression curve can be related to the buckling load by a linear equation of the form

$$P - P_{CR} = A_R(\sigma_E - \sigma_{CR}) \qquad \ldots (1)$$

This expression implies that after local buckling the section behaves as if its effective area against further load is immediately reduced to a given value, A_R, and retains this same effective area thereafter as shown in Fig. 1(b). This reduced effective area, A_R, leads to a reduced second moment of area, I_R, and an altered neutral axis position. The ratio of reduced area A_R to full area A is identical to the ratio of reduced Young's Modulus E^* to Young's Modulus E, ie. E^*/E often used to describe tangent stiffness.

In the case of perfectly manufactured sections at loads not greatly in excess of the local buckling load this gives an accurate description of the section behaviour. In the case of sections with imperfections, or sections loaded far into post-buckling range the tangent stiffness varies with loading. This does not invalidate equation (1) since the tangent stiffness at any stage in the post-buckling range can be related using an equation of this form to some fictitious critical load as shown diagrammatically in Fig.1(c). The fictitious critical load, P_{CR}, and corresponding value of A_R will vary with loading.

Having obtained expressions of this form to govern the compressional and flexural behaviour of a short length of column these can now be used in an equilibrium analysis of the complete column to derive the governing differential equation:-

$$EI_R \frac{d^2\delta}{dx^2} + P\delta = -P(e^*-d) - P_{CR}(e-e^*) \qquad \ldots (2)$$

In this equation δ is the out of plane deflection of the column P_{CR} is the local buckling load of a uniformly compressed section and e, e^* and d define the position of the true neutral axis, the effective neutral axis and the load application point measured from the flange as shown in Fig.2.

This equation can be solved exactly to give the load-deflection relationship in the form

$$\delta = ((e^*-d) + \frac{P_{CR}}{P}(e-e^*))(\sec \frac{\pi}{2}\sqrt{\frac{P}{P_R}} - 1) \qquad \ldots (3)$$

where P_R is the reduced Euler load, ie. $P_R = \frac{\pi^2 EI_R}{L^2}$

For design purposes a more convenient form of equation can be derived from an examination of the physical implications of eq.(2). This examination is carried out in the following section.

Design Analysis

Equation (2) defines the bending behaviour of a column of reduced cross-section effectively under the action of loading as shown in fig. (3). As can be seen the eccentricity of the applied loading is now increased to the value (e*-d) rather than (e-d) for the unbuckled cross-section. A counteracting couple of magnitude $P_{CR}(e^*-e)$ also acts as shown. In the particular case of concentric loading (e=d) then at $P = P_{CR}$ the total moment is zero.

A simple solution to this problem can be obtained by assuming a form for the deflections δ and using the Principle of Minimum Potential Energy to obtain the analysis, as follows:-

Let $\delta = \delta_c \sin \frac{\pi x}{L}$, where δ_c is the deflection at the column centre.

The strain energy of bending is:-

$$u_1 = \int_0^L \frac{EI_R}{2}\left(\frac{d^2\delta}{dx^2}\right)^2 dx = \frac{EI_R}{2}\left(\frac{\pi}{L}\right)^4 \cdot \frac{L}{2}\delta_c^2 \qquad \ldots (4)$$

The potential lost by the loading is:-

$$u_2 = -\frac{P}{2}\int_0^L \left(\frac{d\delta}{dx}\right)^2 dx - (P(e^*-d) - P_{CR}(e^*-e))\left[\frac{d\delta}{dx}\right]_{x=0}^{x=L}$$

ie. $$u_2 = -\frac{P}{2}\left(\frac{\pi}{L}\right)^2 \frac{L}{2}\delta_c^2 + (P(e^*-d) - P_{CR}(e^*-e))\frac{2\pi}{L}\delta_c \qquad \ldots (5)$$

Adding u_1 and u_2 to obtain the total potential energy u and setting $\frac{\partial u}{\partial \delta_c} = 0$ gives the result

$$\delta_c = \frac{4}{\pi}\frac{(P(e^*-d) - P_{CR}(e^*-e))}{\frac{\pi^2 EI_R}{L^2} - P} \qquad \ldots (6)$$

This can be written

$$\delta_c = \frac{4}{\pi}\frac{(P(e^*-d) - P_{CR}(e^*-e))}{P_R - P} \qquad \ldots (7)$$

The bending stress on the compression flange can be obtained from

$$\sigma_B = \frac{My}{I} = EI_R \frac{d^2\delta}{dx^2}\frac{e^*}{I_R} = E\frac{d^2\delta}{dx^2}\cdot e^* \qquad \ldots (8)$$

Now $\frac{d^2\delta}{dx^2} = -\delta_c \sin\frac{\pi x}{L}\left(\frac{\pi}{L}\right)^2 = -\delta_c\left(\frac{\pi}{L}\right)^2$ at the column centre.

Therefore at this point

$$\sigma_B = -E\delta_c\left(\frac{\pi}{L}\right)^2 e^* \quad \text{(compression)}$$

$$\text{or} \quad \sigma_B = \frac{4\pi}{L^2} \frac{(P(e^*-d) - P_{CR}(e^*-e))e^*E}{P_R - P} \qquad \ldots (9)$$

To this must be added the direct stress due to the applied load. From Eq.(1)

$$\sigma_E = \sigma_{CR} + \frac{P - P_{CR}}{A_R} = \frac{P_{CR}}{A} + \frac{P - P_{CR}}{A_R} \qquad \ldots (10)$$

Therefore the flange edge stress due to bending and compression is

$$\sigma_E = \frac{P_{CR}}{A} + \frac{(P-P_{CR})}{A_R} + \frac{4\pi}{L^2} \frac{(P(e^*-d) - P_{CR}(e^*-e))e^*E}{P_R - P} \qquad \ldots (11)$$

In cases where the flange is substantially wider than the lips, or the column is loaded eccentrically towards the flange, eq.(11) gives the maximum stress on the column. For sections with very large lips, or eccentric loading towards the lips, the maximum stress will occur on the lips, and this can be evaluated using a slight modification of eq.(11).

The commonest mode of failure occurs due to material yielding, and this can be estimated by giving σ_E such a value that yield occurs. Failure can also occur in a purely elastic fashion in which the load reaches a maximum value and then reduces with further compression. This can be examined using eq.(7).

Effective Width Criteria

The effects of local buckling for sections with flange relatively wide in comparison to the webs are substantially greater in the flange than in the webs. Moreover the effects of reduced flange width on section bending rigidity and displacement of neutral axis are much greater than the effects of reduced web width. For these reasons reductions in effective widths of the webs can be neglected without incurring any appreciable inaccuracy. Also, if the flanges are much wider than the lips the change in neutral axis at buckling causes the flange stresses to become much greater than those on the lips, so that the lips tend to remain relatively unbuckled and may be assumed fully effective. These assumptions are borne out by rigorous theoretical analysis. Therefore only the flange width need be reduced after local buckling.

There are various effective width expressions which can be used and three will be examined here. These are:-

Case 1) Effective width obtained on the basis of the initial post-buckling behaviour of a perfectly flat square simply supported plate under uniform compression with stress free unloaded edges.

$$\text{ie.} \quad \frac{b_e}{b} = 0.408 + 0.592\frac{\sigma_{CR}}{\sigma_E} \quad \text{(a) for stiffness}$$

$$\text{and} \quad \frac{\overline{b_e}}{b} = 0.26 + 0.74\frac{\sigma_{CR}}{\sigma_m} \quad \text{(b) for strength} \qquad \ldots (12)$$

$$\text{where} \quad \sigma_{CR} = \frac{4\pi^2 E}{12(1-\nu^2)}(t/b)^2.$$

This expression, as do all analytically derived expressions, indicates that for an average edge stress σ_E on the flange there exists a higher maximum edge stress σ_m, occurring at a buckle crest on the flange edge as shown in Fig.(4). Since the load on the plate is obtained from $P = \sigma_E \cdot \frac{b_e}{b} = \sigma_m \cdot \frac{\overline{b_e}}{b}$, then it can easily be shown that

$$\overline{\sigma_E} = \frac{0.26\sigma_m + 0.148\sigma_{CR}}{0.408} \qquad \ldots (13)$$

Thus the edge stress to cause first yield is obtained by setting $\sigma_m = \sigma_Y$ in eq.(13)

The reduced flange area according to eq.(12) is 0.408 times its initial area, and the reduced section properties can be evaluated using this reduced flange area.

Case 2) Effective width obtained using average theoretical values for a lipped channel column.

$$\text{ie.} \quad \frac{b_e}{b} = 0.3 + 0.7\frac{\sigma_{CR}}{\sigma_E} \quad \text{(a) stiffness}$$

$$\frac{\overline{b_e}}{b} = 0.25 + 0.75\frac{\sigma_{CR}}{\sigma_m} \quad \text{(b) strength} \qquad \ldots (14)$$

$$\text{where in this case} \quad \sigma_{CR} = 5.4\frac{\pi^2 E}{12(1-\nu^2)}(t/b)^2$$

These expressions take into account the restraints imposed by the webs on the flange buckling and incorporate a smaller reduced width than the previous expression to take some account of increased buckling effects at high width/thickness ratios.

Case 3) Effective width used in the AISI specification (1). In this case the empirically based effective width is essentially the same for stiffness and strength (although a safety factor is used in the specification for safe load determination). The expression used is

$$\frac{b_e}{t} = 1.9\sqrt{\frac{E}{\sigma_E}}\left(1 - \frac{0.415}{(b/t)\sqrt{\frac{E}{\sigma_E}}}\right) \qquad \ldots (15)$$

This can be shown to be the same as

$$\frac{b_e}{t} = \sqrt{\frac{\sigma_{CR}}{\sigma_E}} - 0.218\,\frac{\sigma_{CR}}{\sigma_E} \qquad \ldots (16)$$

where $$\sigma_{CR} = \frac{4\pi^2 E}{12(1-\nu^2)}\,(t/b)^2.$$

Now at any stress σ_E the flange tangent stiffness can be shown to be

$$\frac{E^*}{E} = 0.5\sqrt{\frac{\sigma_{CR}}{\sigma_E}} \qquad \ldots (17)$$

The corresponding fictitious critical stress $\overline{\sigma_{CR}}$ is given by

$$\overline{\sigma_{CR}} = \sigma_{CR}\,\frac{\left(0.5\sqrt{\frac{\sigma_E}{\sigma_{CR}}} - 0.218\right)}{\left(1-0.5\sqrt{\frac{\sigma_{CR}}{\sigma_E}}\right)} \qquad \ldots (18)$$

Thus expression (15) can be written in the required form of eq.(1), where the fictitious reduced flange area at anystress σ_E is equal to E^*/E, obtained from (17), times the actual flange area, and the fictitious critical stress is related to the actual critical stress σ_{CR} and applied stress σ_E through equation (18)

Example of Analysis

Consider the cross section shown in Fig.(5). The steps required in the analysis, and the results, are detailed here using effective width (1) for illustration as follows:-

1) Determine A, I and e. $A = 360\text{mm}^2$, $I = 188000\ \text{mm}^4$, $e = 16.67$ mm
2) Determine A_R, I_R and e*. $A_R = 241.6\ \text{mm}^2$; $I_R = 139000\ \text{mm}^4$, $e^* = 24.83$ mm
3) Detemine $P_{CR} = \sigma_{CR}.A$. $\sigma_{CR} = 18.05\ \text{N/mm}^2$, $P_{CR} = 6.5$ kN
4) For any given length, L, determine P_R, e.g. L = 5 m, $P_R = 10.975$ kN.
5) Determine $\overline{\sigma_E}$ from (13). $\overline{\sigma_E} = 165.9\ \text{N/mm}^2$.

The load to cause failure is therefore obtained, using eq.(11) from

$$165.9 = \frac{6500}{360} + \frac{(P-6500)}{241.6} + \frac{4\pi}{5000^2} \times 24.83 \times 200 \times 10^3 \frac{(8.16P - 8.16\times 6.5)}{10.975-P}$$

This is quadratic in P and solving gives P = 10.975 kN.

When using this effective width expression, or indeed any effective width expression which has fully reduced properties independent of the flange stress, the failure load will either be that obtained using eq.(11) or the critical load.

When using an expression such as the AISI expression in which the reduced properties vary with σ_E the possibility of elastic failure at loads less than P_{CR} arises. This generally occurs in the region where the Euler load and local buckling load are of similar magnitude, and is largely due to the effects of imperfections, which are taken into account in a generalised way using the AISI expression. Fig.(6) illustrates this behaviour where the load deflection curves for the column are shown on the basis of eq.(7) and the effective width eq. type (3) for various column lengths. As can be seen the column of length 4 metres yields before reaching a maximum elastic load, whereas the longer columns achieve a maximum elastic load before first yield. In these cases the subsequent gradual fall off in load presumes that this can indeed be practically achieved. If the applied loading cannot be gradually reduced to suit then dynamic collapse will follow.

Fig. (7) shows a comparison between the failure loads calculated using the AISI effective width and those using effective width(1). Also shown in this figure is the curve obtained using von Karman's effective width expression, which can be written

$$\frac{b_e}{b} = \sqrt{\frac{\sigma_{CR}}{\sigma_Y}}$$

This is included to illustrate the effects of local imperfections since the AISI effective width expression is a modification of von Karman's equation empirically devised to take the effects of imperfections into account. Comparison of the curves using the AISI expression and von Karman's expression show only a small percentage difference between the two methods except in the region of P_{CR} for the latter case. In this region the maximum difference between failure loads calculated using the two methods is about 30% whereas elsewhere the difference in calculated failure loads is about 5%. This illustrates the well known fact that the greatest effects of imperfections occur in the region where the two different buckling modes, Euler and local, occur simultaneously.

For this geometry of cross section it can be seen that the AISI effective width consistently gives lower results than that obtained on the basis of a square simply supported plate. This is due to the facts that (1) the AISI expression includes imperfections and (2) the latter expression is applicable accurately only in the range σ_E less than about $5\sigma_{CR}$. In spite of this the divergence between the two curves is not excessive. From a general examination of the two effective width criteria over a range of column geometries it is found that if the ratio of flange to web width increases the divergence of results increases and for lower flange/web ratios the curves become closer. Also for lower width to thickness ratios the curves agree more closely. In some cases the effective width case (1) gives lower results than case 3) due to the formulation of the solution despite the fact that the latter effective width is always greater than the former.

Comparison with Experiments

A series of experiments on lipped channel columns was carried out at the University of Strathclyde, using various cross-sectional geometries and loading eccentricities. The tests are described in reference (9) and full details of all columns tested are given in Table 1. Comparisons of the failure loads obtained from test and those calculated using effective width cases (1), (2) and (3) are given in Table 2. The agreement in general is good, and this is illustrated in Fig.8, which shows the variation of the ratio P_{ult}(calculated)/P_{ult}(test) with variation in flange b/t for each case. In this figure, average values were calculated from each set of test results at a given b/t. As can be seen the largest inaccuracies occur for effective width cases (1) and (3) at low (b/t) ratios, due to their neglect of the restraining effects of the webs. Case (2), with its more realistic buckling coefficient, is more accurate in this range.

The AISI effective width expression is consistently conservative in its results, whereas the limitations of the other two expressions are indicated at high b/t ratios. From the results it is evident that the use of the AISI expression, suitably modified to incorporate the increased buckling stress caused by web restraints, will provide consistently accurate ultimate load results using this formulation. Such an expression is given by eq.(16) with the critical stress taken as $\sigma_{CR} = \frac{5\pi^2 E}{12(1-\nu^2)}(t/b)^2$. The results obtained using this expression are shown in Table 2, and depicted graphically in Fig.8 where the agreement with test is seen to be considerably improved.

Comparisons of load-deflection curves produced using the three effective width cases (1), (2) and (3) and those obtained experimentally are shown in Figs. 9, 10 and 11. These indicate that deflections are accurately predicted using case (2) which takes increased buckling load into account. The AISI expression, case (3) consistently overestimates the column deflections and its accuracy in deflection determination is much less than in ultimate load evaluation.

Summary and Conclusions

The method presented permits analysis of column behaviour with a minimum of computational effort. It is quite general in its applicability to any cross-sectional shape, although in this paper only lipped channels have been considered.

The effects of neglecting losses in effectiveness in elements other than the major buckling element does not in general produce any significant discrepancies. For long columns in which the loading is highly offset as failure approaches then buckling is largely confined to one element at loads near failure and the assumption that no losses occur in other elements is accurate. For very short columns there is some inaccuracy in this assumption, but this is counterbalanced by the fact that although a higher I_R is produced by considering one element only to buckle, this also produces a larger eccentricity than would be obtained if all elements are assumed to buckle. These two effects tend to cancel each other, thus producing an accurate estimate of behaviour.

The computed results agree very well with experimental results, and it is found that the AISI expression for effective width gives consistently accurate but conservative predictions. Modification to this expression to increase the critical stress makes for greater accuracy.

APPENDIX I - REFERENCES

1. AMERICAN IRON AND STEEL INSTITUTE. "Specification for the Design of Cold-Formed Steel Structural Members" AISI, New York, N.Y. 1968.

2. DE WOLF, J.T., PEOKOZ, T. and WINTER, G., "Local and Overall Buckling of Cold Formed Members". Proceddings of the ASCE, Vol.100, No.ST10, pp.2017-2036, October 1974.

3. FOK, W.C., RHODES, J. and WALKER, A.C. "Local Buckling of Outstands in Stiffened Plates". Aeronautical Quarterly, Vol.XXVII, May 1976.

4. FOK, W.C., WALKER, A.C. and RHODES, J. "Buckling of Locally Imperfect Stiffeners in Plates". Proceedings of the ASCE, Vol. 103, No. EM5, pp.895-911, October 1977.

5. GRAVES SMITH, T.R. "The Ultimate Strength of Locally Buckled Columns of Arbitrary Length". Thin Walled Steel Constructions. Their Design and Use in Building. Symposium at University College of Swansea, 11-14 September, 1967.

6. KONIG, J. and THOMASSON, P.O. "Thin-Walled C-Shaped Panels Subject to Axial Compression or to Pure Bending". International Conference on Thin Walled Structures, University of Strathclyde, Glasgow, Scotland, 3-6 April 1979.

7. LOUGHLAN, J. and RHODES, J. "Interaction Buckling of Lipped Channel Columns". Conference on Stability Problems in Engineering Structures and Components, University College, Cardiff, 12-14 September, 1978.

8. LOUGHLAN, J. and RHODES, J. "The Interactive Buckling of Lipped Channel Columns under Concentric or Eccentric Loading". International Conference on Thin Walled Structures, University of Strathclyde, Glasgow, Scotland, 3-6 April, 1979.

9. LOUGHLAN, J. "Mode Interaction in Lipped Channel Columns under Concentric or Eccentric Loading". PhD Thesis, University of Strathclyde, Glasgow, Scotland, December 1979.

10. NEUT, A. van der. "The Interaction of Local Buckling and Column Failure of Thin Walled Compression Members". Proceedings of the Twelth International Congress of Applied Mechanics, Stanford University, 26-31 August, 1968. Springer-Verlag Berlin, Heidelberg, New York 1969.

11. RHODES, J. and HARVEY, J.M. "Interaction Behaviour of Plain Channel Columns under Concentric or Eccentric Loading". Second International Colloquium on the Stability of Steel Structures, Liege, PP.439-444, 13-15 April, 1977.

12. WANG, S.T. and TIEN, Y.L. "Post Local Buckling Behaviour of Thin Walled Columns". Proceedings of Second Speciality Conference on Cold Formed Steel Structures, St. Louis, Missouri, pp.53-81, 1973.

APPENDIX II - NOTATION

The following symbols are used in this paper:

A = Full cross sectional area
A_R = Reduced cross sectional area
E = Young's modulus of elasticity
E^* = Reduced Young's modulus of elasticity
I = Second moment of area
I_R = Reduced second moment of area.
L = Column length
P = Axial load on column
P_{CR} = Critical local buckling load
$\overline{P}_{CR}$ = Fictitious critical local buckling load
P_R = Reduced Euler load
u = Total potential energy
u_1 = Strain energy of bending
u_2 = Loss in potential of loading
b = Width of flange
b_e = Effective width for stiffness
b_ℓ = Width of lip
b_w = Width of web
$\overline{b}_e$ = Effective width for strength
d = Load application point measured from the flange
e = Position of neutral axis measured from flange
e^* = Effective position of neutral axis after local buckling
t = Section plate thickness
δ = Column deflection
δ_c = Central deflection of column
ν = Poisson's ratio
σ_B = Bending stress
σ_{CR} = Critical local buckling stress
$\overline{\sigma}_{CR}$ = Fictitious critical local buckling stress
σ_E = Average flange edge stress
$\overline{\sigma}_E$ = Average flange edge stress to cause first yield
σ_m = Maximum flange edge stress
σ_y = Material yield stress
r = Minimum radius of gyration of section

TABLE 1

TEST COLUMN DIMENSIONS AND LOADING ECCENTRICITY

Column No.	e-d (mm)	b (mm)	b_w (mm)	b_ℓ (mm)	t (mm)	L (mm)
1	7.43	101.55	50.57	18.85	0.81	1828.80
2	7.47	101.12	50.50	19.24	0.79	1219.20
3	10.22	102.74	62.77	25.44	0.79	1828.80
4	10.25	101.98	62.79	25.40	0.81	1524.00
5	10.34	101.63	62.99	25.74	0.79	1219.20
6	1.67	127.86	50.60	18.68	0.79	1828.80
7	1.68	126.39	50.47	18.86	0.79	1524.00
8	1.69	126.47	50.55	19.14	0.80	1219.20
9	4.68	127.79	62.71	25.42	0.80	1828.80
10	4.72	127.36	63.02	25.50	0.80	1524.00
11	4.73	126.75	62.92	25.58	0.81	1219.20
12	4.63	151.92	50.75	18.95	0.81	1828.80
13	4.66	152.20	50.60	19.66	0.81	1524.00
14	4.61	151.74	50.47	19.02	0.81	1219.20
15	0.0	153.95	62.79	25.37	0.80	1828.80
16	0.0	153.95	62.89	25.60	0.81	1524.00
17	0.0	152.02	62.97	25.57	0.80	1219.20
18	5.58	178.03	50.17	18.86	0.80	1828.80
19	5.64	177.17	50.47	18.94	0.80	1524.00
20	5.70	177.67	50.50	19.58	0.81	1219.20
21	4.03	178.31	62.94	25.23	0.79	1828.80
22	4.03	178.33	62.97	25.32	0.80	1524.00
23	4.08	176.53	63.02	25.85	0.80	1219.20
24	0.0	152.30	49.28	17.74	1.64	1828.80
25	2.11	152.25	61.72	24.58	1.66	1828.80
26	2.11	152.04	61.67	24.74	1.68	1524.00
27	2.12	151.38	61.82	24.86	1.66	1219.20
28	2.69	178.05	49.25	17.99	1.64	1828.80
29	2.70	177175	49.38	17.97	1.65	1524.00
30	2.70	176.10	49.10	18.10	1.65	1219.20
31	0.0	178.23	61.85	24.62	1.63	1828.80
32	0.0	177.93	61.62	24.77	1.64	1524.00
33	0.0	176.73	61.98	25.71	1.64	1219.20

TABLE 2

COMPARISON WITH EXPERIMENTAL ULTIMATE LOADS

Column No.	P_{ult} (kN) Exp.	P_{ult} (kN) (1)	% Error	P_{ult} (kN) (2)	% Error	P_{ult} (kN) (3)	% Error	MOD AISI P_{ult} (kN)	MOD AISI % Error	$\frac{\sigma_Y}{\sigma_{CR}}$	$\frac{b}{t}$
1	13.90	12.64	-9.1	15.24	+9.6	13.13	-5.5	13.83	-0.5	5.62	127.5
2	16.01	14.12	-11.8	15.88	-0.8	15.29	-4.5	16.16	+0.9	5.62	127.5
3	15.66	15.2	-2.9	16.92	+8	16.42	+4.9	17.39	+11.0		
4	16.81	15.78	-6.1	17.74	+5.5	17.33	+3.1	18.36	+9.2		
5	18.24	16.2	-11.2	18.43	+1	18.11	-0.7	19.18	+5.2		
6	16.90	15.8	-6.5	16.4	-3	15.02	-11.1	16.13	-4.6	8.79	159.4
7	17.66	16.8	-4.9	17.8	+0.8	16.47	-6.7	17.71	+0.3		
8	19.17	17.62	-8.1	18.95	-1.1	17.73	-7.5	19.06	-0.6		
9	19.30	18.09	-6.3	19.63	+1.7	18.7	-3.1	19.82	+2.7		
10	20.33	18.79	-7.6	20.59	+1.8	19.97	-1.8	20.98	+3.2		
11	20.68	19.33	-6.5	21.39	+3.4	20.71	+0.15	21.95	+6.1		
12	14.90	14.43	-3.2	15.14	+1.6	13.52	-9.26	14.28	-4.2	12.22	188.6
13	15.70	15.31	-2.5	16.32	+3.9	14.7	-6.37	15.69	-0.1		
14	17.12	16.03	-6.4	17.32	+1.2	15.73	-8.1	16.8	-1.9		
15	21.80	21.85	+0.2	23.12	+6.1	20.82	-4.5	22.17	+1.7		
16	23.04	22.61	-1.9	24.27	+5.3	22.09	-4.1	23.51	+2		
17	23.62	23.21	-1.7	25.16	+6.5	23.14	-2.0	24.61	+4.2		
18	13.94	14.19	+1.8	14.56	+4.4	12.44	-10.76	13.27	-4.8	17.04	222
19	15.08	15.05	-0.2	15.68	+4.0	13.48	-10.61	14.39	-4.6		
20	16.32	15.76	-3.4	16.64	+2.0	14.39	-11.83	15.38	-5.8		
21	17.19	18.86	+9.7	19.8	+15.2	17.26	+0.4	18.34	+6.7		
22	19.64	19.54	-0.5	20.75	+5.7	18.22	-7.23	19.37	-1.4		
23	18.44	20.09	+8.9	21.54	+16.8	19.04	+3.2	20.23	+9.7		
24	65.83	52.63	-20.1	58.52	-11.1	49.32	-25.1	53.41	-18.9	2.90	91.6
25	70.95	61.52	-13.3	70.58	-0.5	61.35	-13.53	66.04	-6.9		
26	72.95	63.93	-12.4	74.05	+1.5	65.04	-10.8	69.98	-4.1		
27	73.84	65.73	-11.0	76.63	+3.8	67.94	-7.99	73.03	-1.1		
28	51.15	44.32	-13.4	47.63	-6.9	42.65	-16.62	45.98	-10.1	4.05	108.2
29	56.27	47.68	-15.3	52.18	-7.3	47.13	-16.24	50.94	-9.5		
30	60.27	50.26	-16.6	55.79	-7.4	50.88	-15.58	55.04	-8.7		
31	75.39	61.81	-18.0	68.92	-8.6	62.14	-17.58	67.19	-10.9		
32	75.84	63.96	-15.7	72.18	-4.8	65.84	-13.19	71.14	-6.2		
33	80.29	65.53	-18.4	74.58	-7.1	68.72	-14.41	74.15	-7.6		

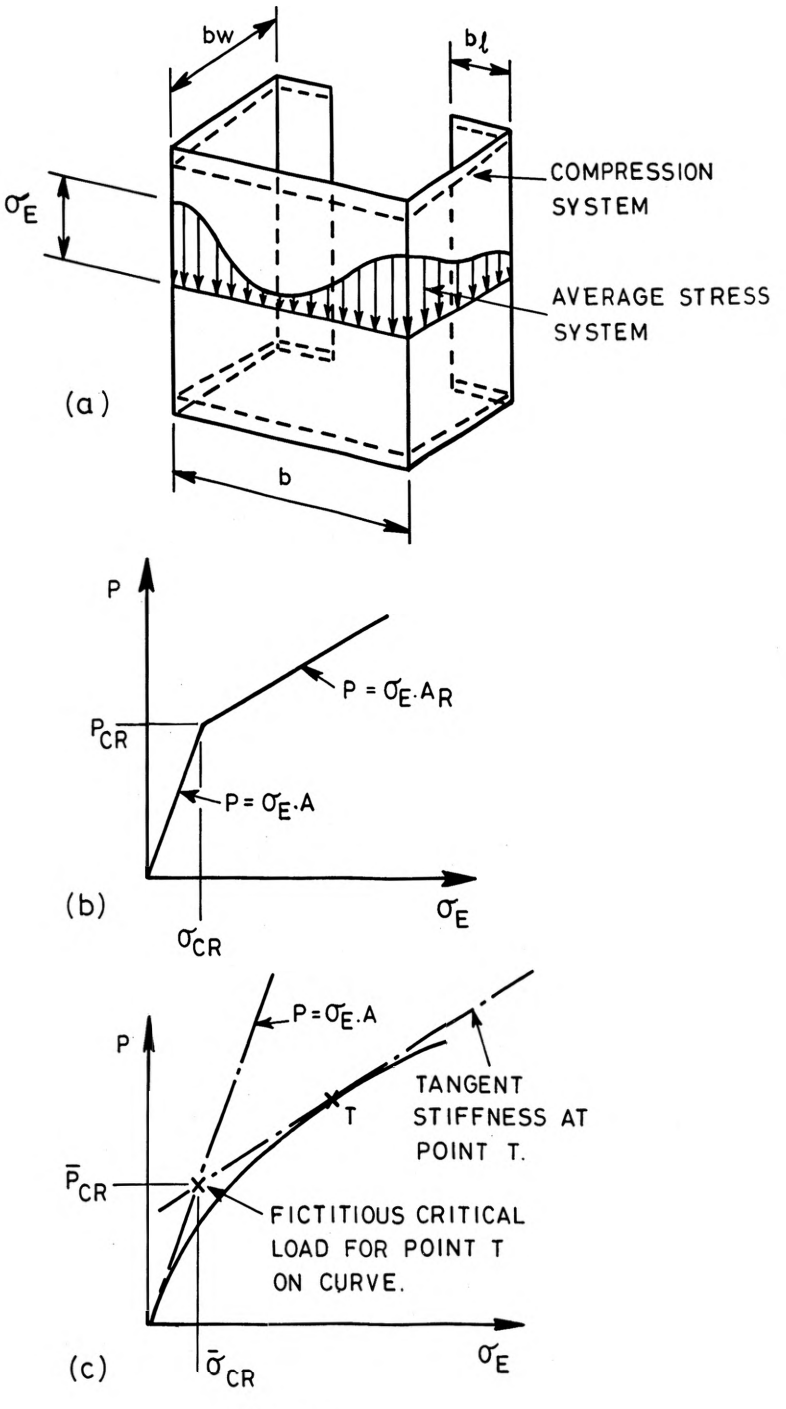
bw
bℓ
σE
COMPRESSION SYSTEM
AVERAGE STRESS SYSTEM
(a)
b
P
PCR
P = σE·AR
P = σE·A
(b)
σE
σCR
P = σE·A
P
TANGENT STIFFNESS AT POINT T.
T
P̄CR
FICTITIOUS CRITICAL LOAD FOR POINT T ON CURVE.
(c)
σ̄CR
σE

FIG. 1

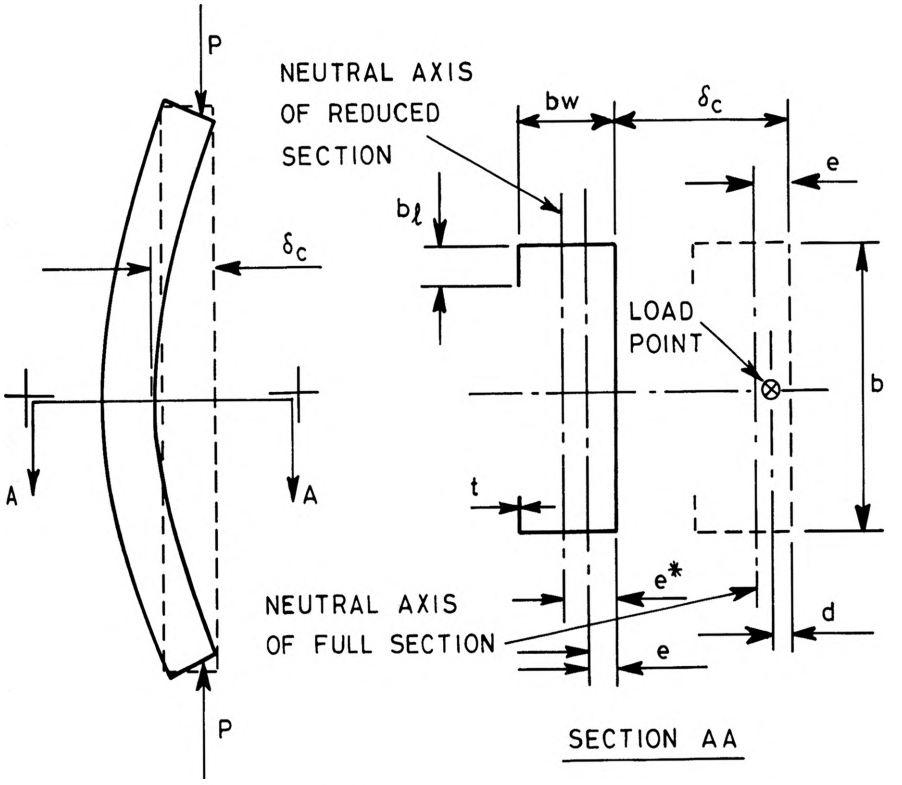
P
NEUTRAL AXIS
OF REDUCED
SECTION
bw
δ_c
e
b_ℓ
δ_c
LOAD
POINT
b
A
A
t
e^*
NEUTRAL AXIS
OF FULL SECTION
d
e
P
SECTION AA

FIG. 2.

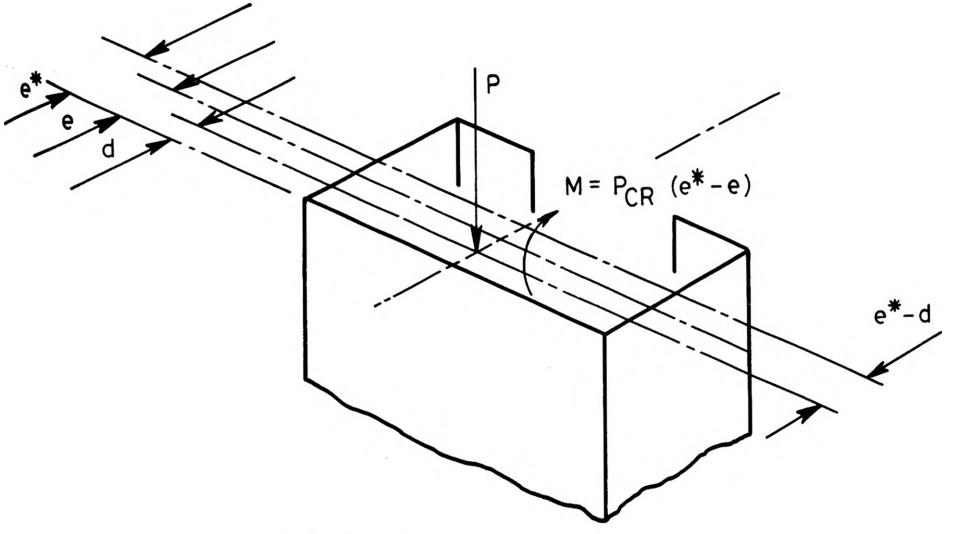
e^*
e
d
P
$M = P_{CR}\ (e^* - e)$
$e^* - d$

FIG. 3.

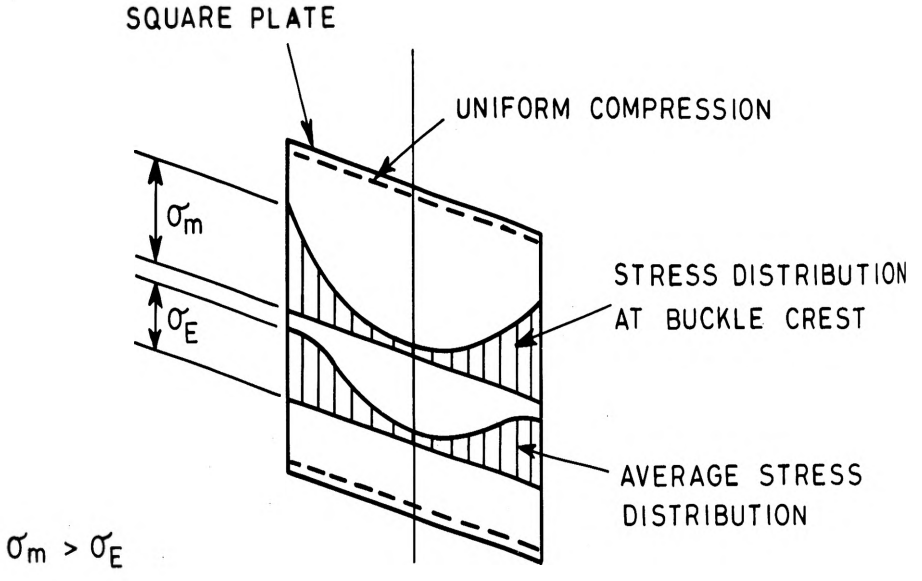
SQUARE PLATE
UNIFORM COMPRESSION
σ_m
σ_E
STRESS DISTRIBUTION
AT BUCKLE CREST
AVERAGE STRESS
DISTRIBUTION
$\sigma_m > \sigma_E$

FIG 4

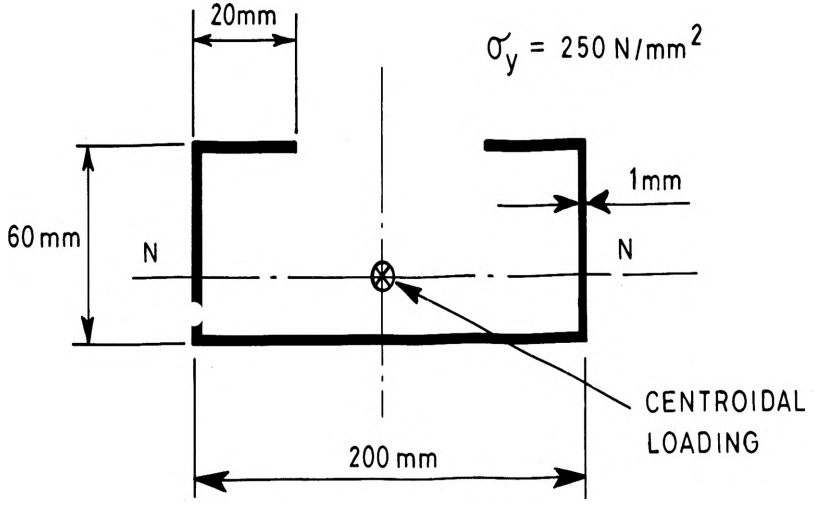
20mm
$\sigma_y = 250\ N/mm^2$
1mm
60 mm
N
N
CENTROIDAL
LOADING
200 mm

FIG. 5

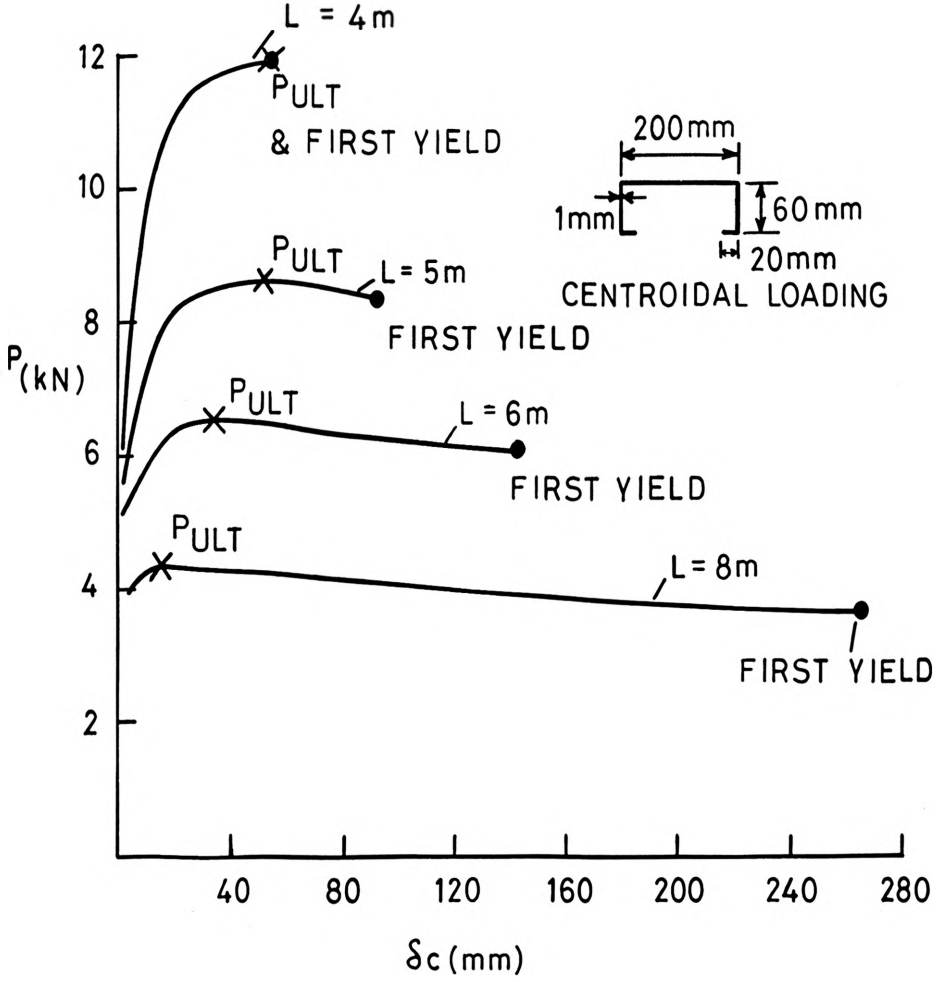

FIG 6. LOAD-DEFLECTION CURVES USING AISI EFFECTIVE WIDTHS

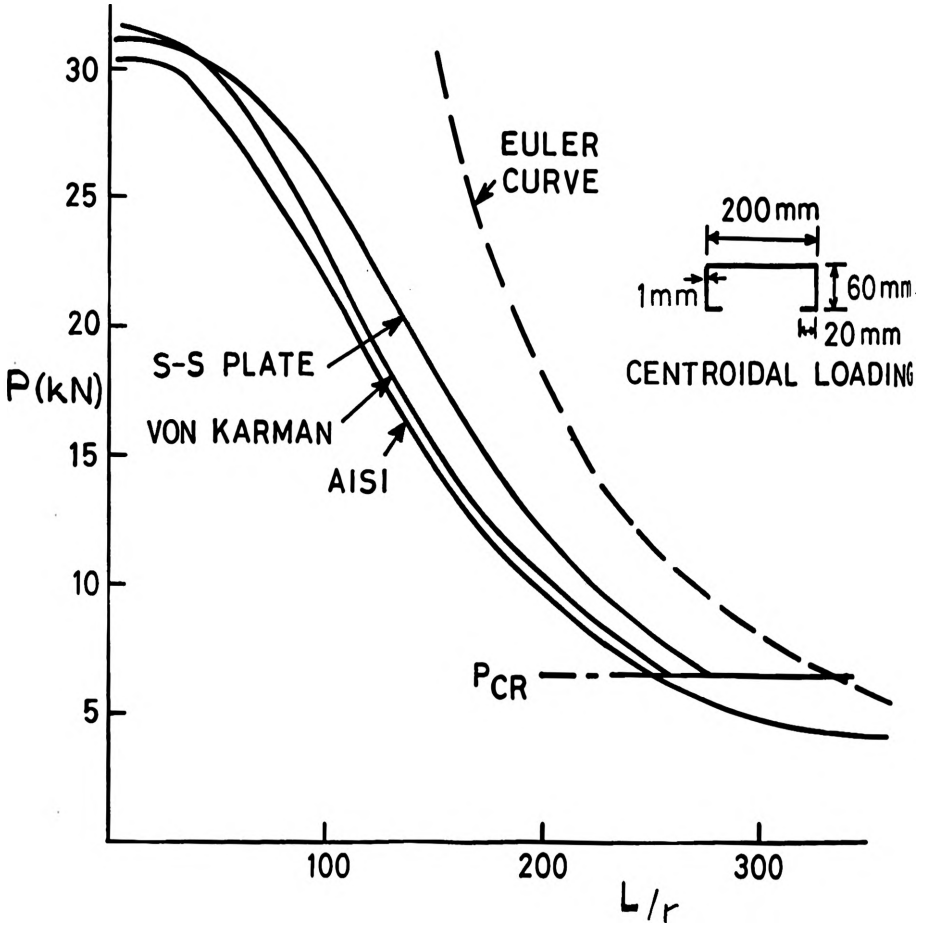

FIG 7. COMPARISON OF DIFFERENT EFFECTIVE WIDTH APPROACHES FOR TYPICAL COLUMN CROSS-SECTION

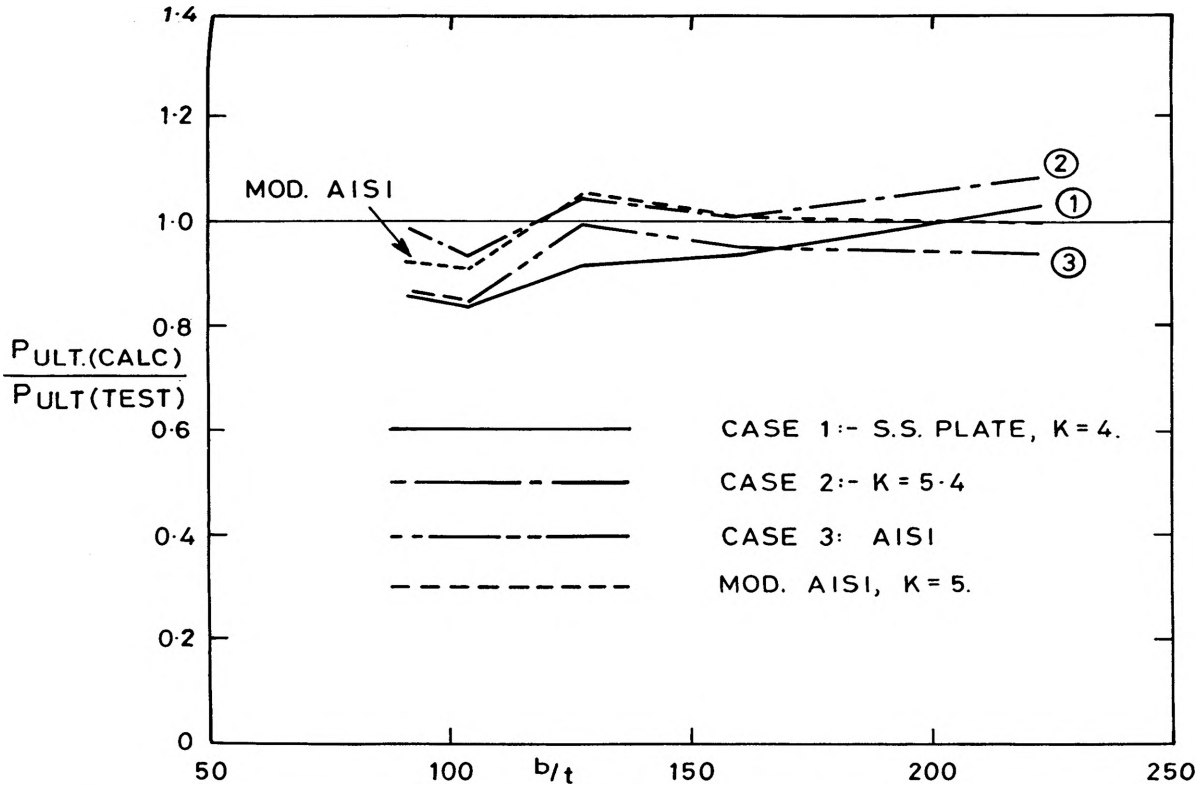

FIG. 8 COMPARISON WITH EXPERIMENT FOR THE DIFFERENT EFFECTIVE WIDTH CASES.

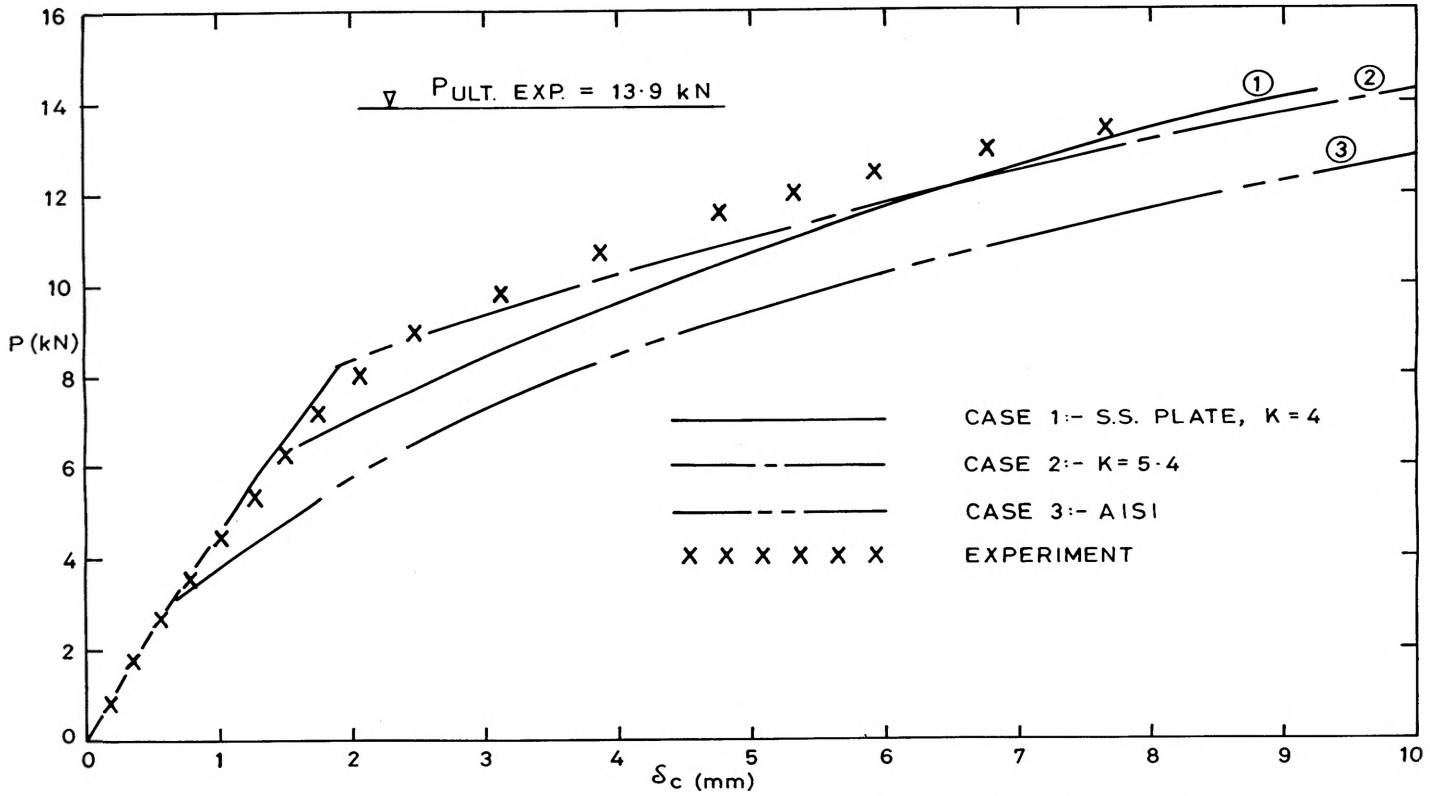

FIG 9. LOAD DEFLECTION CURVES FOR COLUMN Nº 1

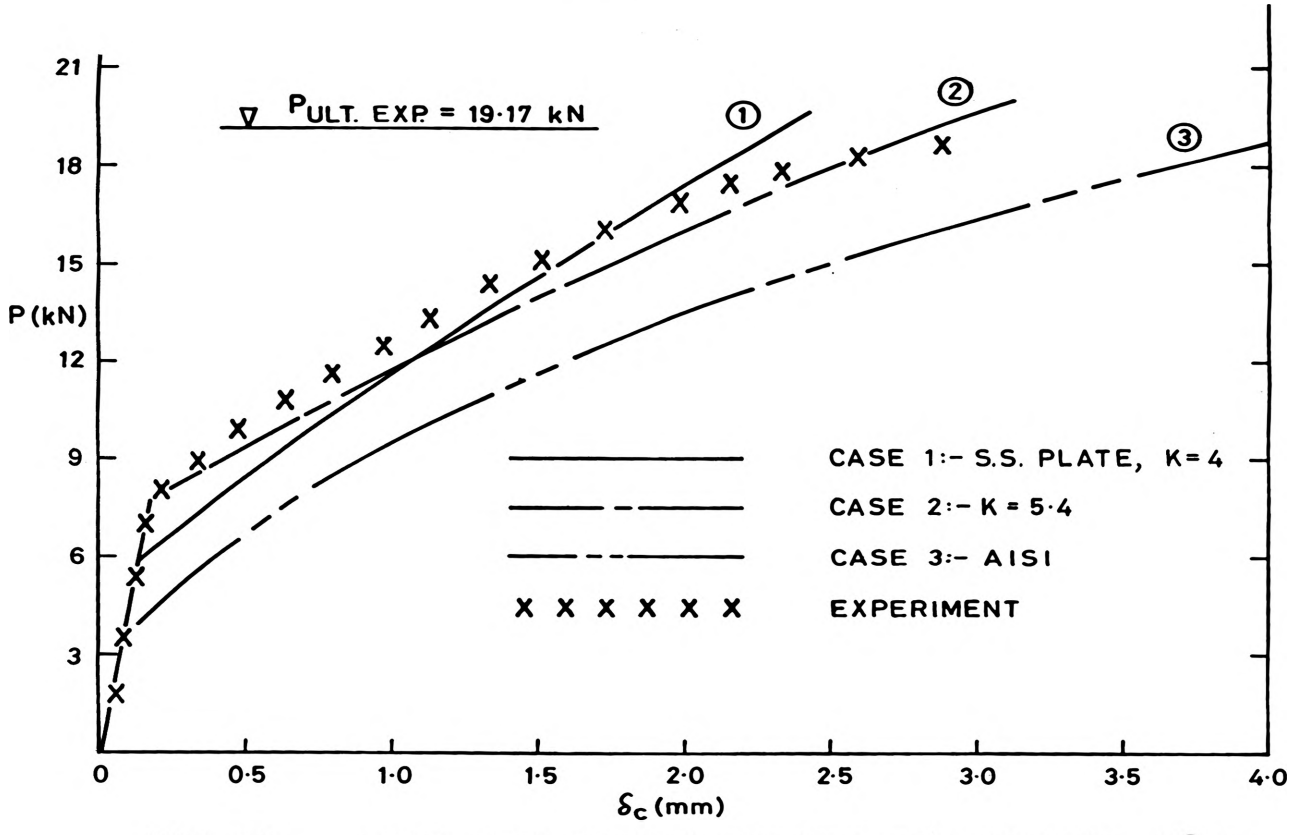

FIG. 10. LOAD DEFLECTION CURVES FOR COLUMN Nº 8.

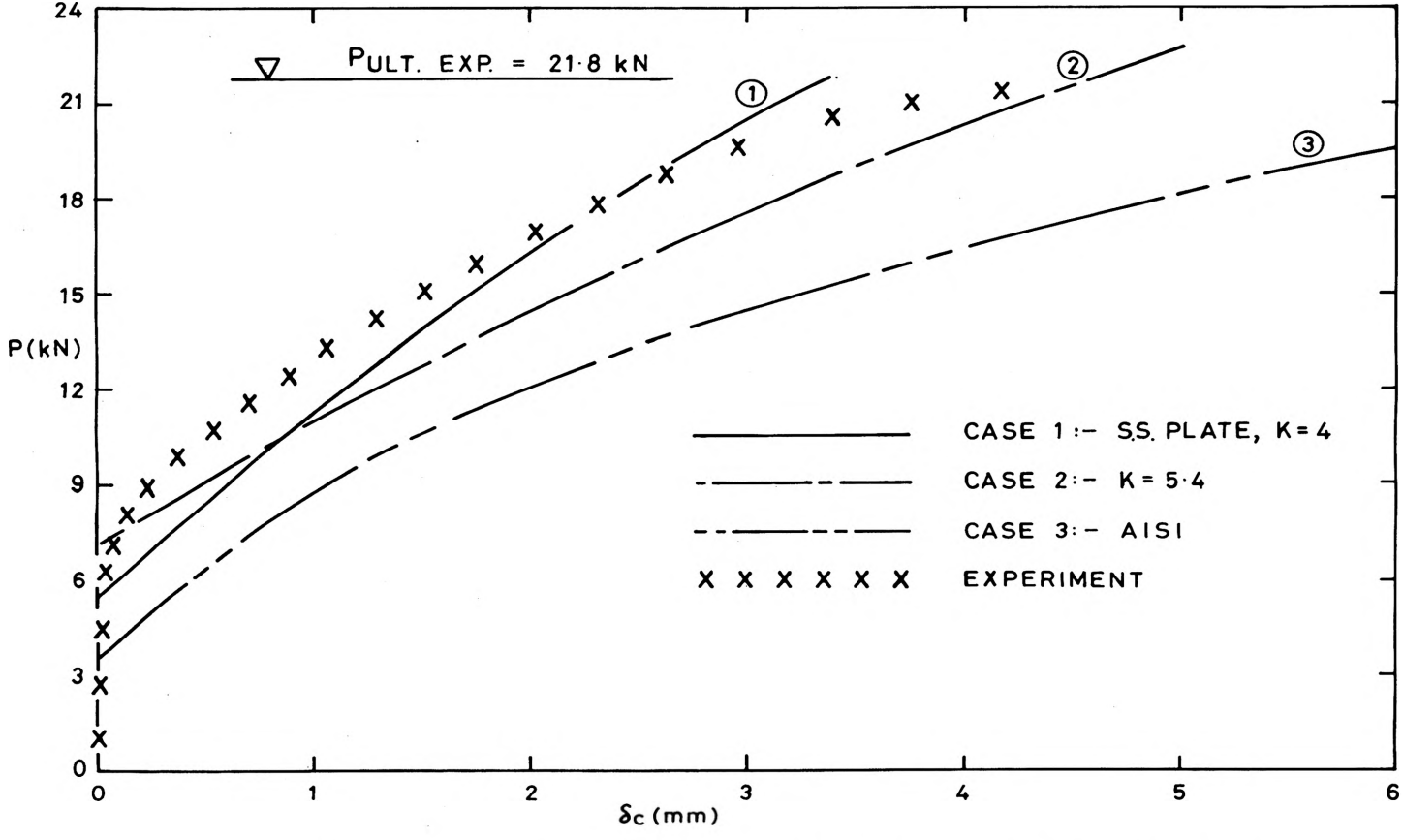

FIG 11. LOAD DEFLECTION CURVES FOR COLUMN Nº 15